# *In-situ* acidification of electrosterically dispersed alumina suspensions: Effect of coagulant structure

JON G.P. BINNER*
*Institute of Polymer Technology & Materials Engineering, Loughborough University, Leicestershire, LE11 3TU, UK; Formerly of the Department of Materials Engineering & Materials Design, The University of Nottingham, UK*

ANDREW M. MCDERMOTT
*British Ceramic Tile, Newton Abbot, UK; Formerly of the Department of Materials Engineering & Materials Design, The University of Nottingham, UK*

**Published online:** 17 February 2006

The effect of the acidification arising from the hydrolysis of a range of carboxylic acid derivative compounds on the behaviour of electrosterically dispersed alumina slurries has been studied and it has been demonstrated that they can be successfully coagulated in a time-dependent manner. The inherent coagulation rate is determined by a number of factors, including the precise molecular composition and conformation of the coagulant, as well as its concentration and the suspension temperature. For the cyclic compounds, the size of the ring exhibits a significant influence on the coagulation rate with factors that affect the ground and transition state energies responsible for the observed trends. The nature of the atom bonded to the carbonyl carbon also influences the coagulation rate, with substituent hydroxyl groups accelerating the process. These side group entities can adopt a range of spatial arrangements, however certain conformations result in the formation of hydrogen bonds with the attacking water nucleophile. These favourable interactions stabilise the transition state and hence reduce the activation energy. 

## 1. Introduction

Colloidal powder processing is now a widely used method of producing high integrity ceramic components; there is an abundance of literature outlining the principles involved [1–4]. There are a number of different approaches that can be adopted but they almost all rely on starting with a well dispersed, highly homogenous suspension and then consolidating it into a green body possessing the required shape, high packing density and some degree of handling strength, without introducing strength limiting defects into the microstructure [2]. Consolidation may be due to solvent removal, as in slip or freeze casting [5, 6], the creation of a network that traps the particles, as in gel casting [7], or modifying the dominant interparticle force, as in direct coagulation casting [8]

The major disadvantage of removing the suspending media is that solvent inevitably becomes trapped within the body during the latter stages of the process whilst with processes like gel casting there is the problem of binder removal since relatively large amounts can be involved. Whilst consolidation by manipulating the interparticle forces has conventionally resulted in the formation of a flocculated network, coagulated bodies are more desirable because they permit the particles to slide around after initial contact under the influence of Brownian motion, rather like a lubricating layer. Consequently the green bodies possess higher packing densities, similar to those obtained from dispersed suspensions, a uniformity which reflects the homogeneity of the colloidal state and a viscosity lower than the corresponding flocculated systems [9–15].

Coagulated networks are formed when strong interparticle repulsions are generated at close separations [16]. As the particles approach one another the van der Waals attractive potential dominates until close range when the action of the repulsive force prevents the particles from

*Author to whom all correspondence should be addressed.
0022-2461 
DOI: 10.1007/s10853-006-4438-1

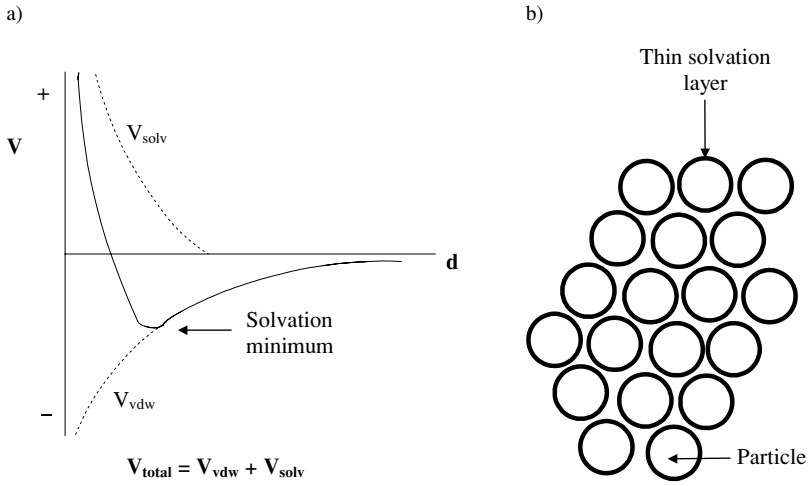


*Figure 1* (a) Interparticle potential-separation curve for a coagulated system. Upon close approach the particles fall into a solvation minimum, at which point the particles remain sufficiently far enough apart that they do not touch each other. (b) Schematic representation of the non-touching, attractive network that forms in coagulated systems.

falling into the deep primary minimum, Fig. 1. Although these repulsive forces have a short range they can be substantial at high phase volumes and so at the equilibrium separation the particles reside in a shallow minimum where the attractive potential is less effective than in the flocculated case.

The repulsive interaction is typically generated through solvation forces or steric effects. For example, coagulation can be achieved via the addition of a salt to a dispersed suspension. For electrosteric dispersion the electrostatic charges on the polyelectrolyte chains are shielded, allowing them to coil and act as uncharged polymers. Thus the salt reduces the solvent quality and hence enhances adsorption [17]. Upon suppression of the diffuse double layer, steric forces dictate the stability of the suspension. If the adsorbed layer is relatively thin, attraction will dominate due to van der Waals forces and the suspension will become more viscous [18, 19]. Time dependent effects such as configurational changes to the adsorbed layer may affect suspension stability and it can be difficult to distribute the salt uniformly through the precursor dispersed suspension since coagulation can occur immediately and locally on introduction of the salt [16].

Graule et al [8, 20, 21] have patented the Direct Coagulation Casting method for the production of complex shaped, high strength, high reliability ceramic components. The consolidation step is based on the destabilisation of a high solids loading electrostatically stabilised suspension, destabilisation being brought about by the *in-situ* time dependant formation of potential determining or indifferent ions from initially inactive compounds utilising enzyme catalysed reactions. For example, electrostatically stabilised suspensions can be coagulated due to a change in ionic strength according to:

$$H_2NCONH_{2\,(aq)} + 2H_2O_{(l)} \xrightarrow{\text{urease}} {CO_3}^{2-}{}_{(aq)} + 2NH_4^+{}_{(aq)}$$

Essentially this reaction is the same as that utilised by Franks [22] in the Vibraforming route, although in that case heat was used rather than enzymes to obtain appreciable reaction rates. A shift in pH from alkaline to neutral pH is achievable using the glucose, glucoseoxidase system [21]. The strength of the resultant green body has been found to be higher than when an increase in salt concentration is used to achieve coagulation as a result of the short range hydration forces acting between the particles in the latter case [22].

The hydrolysis of carboxylic acid derivative compounds has been intensively investigated for many decades, especially in the biochemical and biological sense [23–29]. When mixed with water hydroxy carboxylic acid forms, which partially dissociates and subsequently acidifies the solution; the amount dissociated being dependent upon the characteristics of the acid in question and the original pH of the medium. This change in pH can be used to control the level of charge on the ceramic particles in an aqueous suspension and hence the degree of dispersion. By activating the pH change *in-situ* at a controllable rate, the viscosity of the suspension can be manipulated so that it is low during casting into a mould and then increases rapidly to a point where the cast body is rigid enough to be de-moulded. This offers the potential to produce complex-shaped ceramics fast and economically.

## 2. Experimental

Preparation of the initial dispersed suspensions followed the procedure developed by Davies & Binner [30]. Appropriate quantities of deionised water (±0.01 g) and Dispex A40[1] (±0.003 g) were mixed until the dispersant was uniformly distributed and then A-16SG alumina[2]

[1] Allied Colloids, Bradford, UK.
[2] Alcoa Manufacturing (GB) Ltd, Worcester, UK.

TABLE I List of the coagulants utilised within the research

| Coagulants | |
|---|---|
| N-ethylacetamide | ethylacetate |
| $\gamma$-butyrolactone | succinic anhydride |
| $\beta$-propyrolactone | $\delta$-valerolactone |
| $\varepsilon$-caprolactone | $\gamma$-valerolactone |
| $\gamma$-caprolactone | $\gamma$-octanoiclactone |
| $\alpha$-methyl-$\gamma$-buyrolactone | ($\pm$)-$\alpha$-hydroxy-$\gamma$-lactone |
| D-erythronic-$\gamma$-lactone | L-mannonic-$\gamma$-lactone |
| D-gulonic-$\gamma$-lactone | L-gulonic-$\gamma$-lactone |
| $\alpha$-D-glucoheptonic-$\gamma$-lactone | D-glucono-$\delta$-lactone |
| $\alpha$-acetyl-$\gamma$-butyrolactone | |

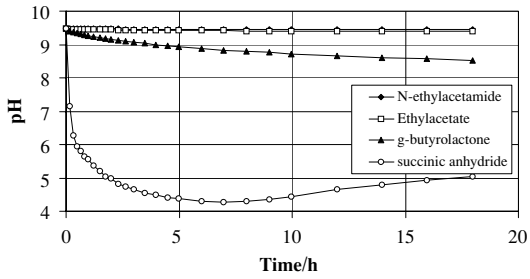


*Figure 2* Time dependent variation in suspension pH, following the introduction of $2.50 \times 10^{-5}$ mol g$^{-1}$ of selected carboxylic acid derivatives to a standard dispersed suspension at a temperature of 25 $\pm$ 1°C.

($\pm$0.01 g) blended in until an homogenous suspension resulted. Since Dispex A40 is an aqueous solution, the actual quantity of ammonium polyacrylate (NHPA) used corresponded to only 37.6 wt% of the amount of dispersant added. In order to account for this the quantity of NHPA utilised was recorded in terms of the mass added per gram of alumina powder, denoted mg g$^{-1}$ hereafter. Furthermore, all associated water was allowed for during the batching process calculations. Unless otherwise stated the composition of the initial dispersed suspensions was 81 wt% alumina and 1.4 mg g$^{-1}$ ammonium polyacrylate.

Following mixing the slurries were covered to avoid contamination and left to stand at room temperature for 1 h to allow adsorption of the dispersant onto the alumina. In order to breakdown any soft agglomerates, the slurry was then subjected to ultrasonic agitation produced by a Kerry ultrasound unit[3] for 90 seconds. The vibrational output was at a frequency of 20 kHz and a power level of 150 W. In order to reduce subsequent water evaporation, the samples were covered with Nescofilm[4] and cooled in a refrigerator for 1 h. The dispersed suspensions were stirred and then placed in a 60 $\pm$ 10 mm Hg vacuum for 1 h in order to remove as much of the entrapped air as possible. Finally the suspensions were re-sealed and allowed to equilibrate in a refrigerator for 24 h.

The effect of a wide variety of coagulants at various concentrations and temperatures was investigated. The former allowed the reaction rate and the latter the activation energy to be calculated. As a preliminary experiment the solubility in water of all potential coagulants was verified and only compounds displaying a high solubility were used, Table I, because any phase separation occurring between aqueous and organic phases would unduly complicate the results and probably be commercially impractical. To ease comparison, all additions are denoted by the number of moles of coagulant added per gram of unit mass of suspension, mol g$^{-1}$.

For the coagulation experiments the dispersed suspension was covered with Nescofilm to minimise evaporation and partially immersed in a gently agitated water bath to achieve constant temperature conditions. The cover was removed and the coagulant thoroughly blended into the suspension for one minute prior to pH and temperature probes being inserted and the cover replaced. The pH measurements allowed the kinetics of the coagulation process to be established as well as providing information about the extent of pH change. The initial rate of the reaction was determined by measuring the concentration of $H^+$ that had formed 5 minutes after the additive had been introduced into the dispersed suspension.

All pH measurements were taken using a Jenway 3020 pH meter[5] fitted with a spear-tip glass electrode[6] that was specifically designed to minimise the blockage problems associated with working with concentrated suspensions. The probe was calibrated and checked before use with standard buffer solutions at 25.0°C. An automatic temperature compensation (ATC) probe and a PC that acted as a data logger automatically recorded the temperature and pH every 10 seconds. After each experiment the electrode and ATC probe were thoroughly rinsed in deionised water and immersed in buffer solutions to eliminate excessive electrode drift. The accuracy of all pH readings was $\pm$0.1 pH units.

## 3. Results

In the following subsections, the effectiveness of the coagulants are depicted graphically under standard test conditions of $2.5 \times 10^{-5}$ mol g$^{-1}$ of coagulant at an isothermal temperature of 25°C whilst the calculated results of the

[3]Kerry Ultrasonics Ltd., Hitchin, Hertfordshire, UK.
[4]Nescofilm$^{TM}$, Nippon Shoji Kaisha Ltd., Osaka, Japan.
[5]Jencon Scientific Ltd., Leighton Buzzard, Bedfordshire, UK.
[6]pH electrode reference number 924002, Jencon Scientific Ltd., Leighton Buzzard, Bedfordshire, UK.

TABLE II Coagulation rate constants at 25$\pm$1°C for various carboxylic acid derivatives

| Coagulant | Leaving group | Coagulation rate constant at 25°C / s$^{-1}$ |
|---|---|---|
| Succinic anhydride | R-$CO_2^-$ | $4.94 \times 10^{-5}$ |
| $\gamma$-butyrolactone | $^-$OR | $2.03 \times 10^{-9}$ |
| Ethylacetate | $^-$OR | $2.62 \times 10^{-10}$ |
| N-ethylacetamide | $^-NH_2$ | $1.75 \times 10^{-11}$ |

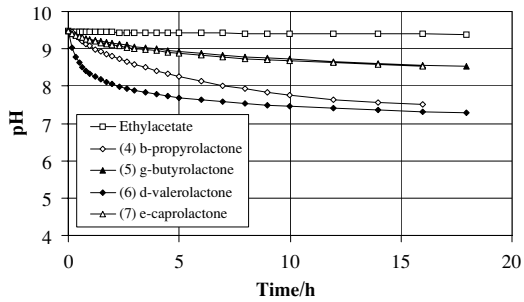


*Figure 3* Effect of lactone ring size on the time dependent variation of suspension pH. Note that when referring to the ring size (number in brackets), all atoms within the ring are considered.

reaction kinetics and activation energies, from the effect of concentration and temperature respectively, are tabulated.

### 3.1. Carboxylic acid derivative sub-classification

The time dependent effects of hydrolysis for a representative member of each of the different groups ofcarboxylic acid derivatives investigated are presented in Fig. 2 and Table II. The coagulants shown were selected such that the molecular backbone contained an identical number of carbon atoms, with differences only arising from the functional group possessed. The results demonstrate that the extent of pH change and the rate of coagulation exhibited is diverse. Insignificant differences were observed for the amide and ester compounds, however a rapid change was noted for the acid anhydride with the lactone showing an intermediate response.

### 3.2. Ring size

The effect of ring size for lactone coagulants is presented in Fig. 3 and Table III. In this case, the coagulants shown have been selected such that they possess no side groups and differ only by the number of atoms within the ring. Note that when referring to the ring size, all atoms within the ring are considered. For example the 5-membered ring compound $\gamma$-butyrolactone comprised 4 carbon atoms and an oxygen atom. For comparison, data for the linear ester, ethylacetate, is also shown in the figure.

TABLE III Coagulation rate constants at 25±1°C and activation energies for lactones of differing ring size

| Lactone | Ring size | Coagulation rate constant at 25°C / $s^{-1}$ | Activation energy / kJ $mol^{-1}$ |
|---|---|---|---|
| $\beta$-butyrolactone | 4 | $1.69 \times 10^{-8}$ | 89 |
| $\gamma$-butyrolactone | 5 | $2.03 \times 10^{-9}$ | 95 |
| $\delta$-valerolactone | 6 | $6.07 \times 10^{-8}$ | 81 |
| $\varepsilon$-caprolactone | 7 | $2.01 \times 10^{-9}$ | 96 |

TABLE IV Coagulation rate constants at 25±1°C and activation energies for lactones possessing different hydroxyl containing side groups.

| Lactone | Coagulation rate constant at 25°C / $s^{-1}$ | Activation energy/kJ $mol^{-1}$ |
|---|---|---|
| 5-membered ring | | |
| $\gamma$-butyrolactone | $2.03 \times 10^{-9}$ | 94 |
| (±)-$\alpha$-hydroxy-$\gamma$-butyrolactone | $7.66 \times 10^{-8}$ | 72 |
| D-erythronic-$\gamma$-lactone | $1.18 \times 10^{-8}$ | 68 |
| L-mannonic-$\gamma$-lactone | $1.71 \times 10^{-7}$ | 70 |
| D-gulonic-$\gamma$-lactone | $1.69 \times 10^{-7}$ | 68 |
| L-gulonic-$\gamma$-lactone | $1.69 \times 10^{-7}$ | 69 |
| $\alpha$D-glucoheptonic-$\gamma$-lactone | $1.39 \times 10^{-6}$ | 63 |
| 6-membered ring | | |
| D-glucono-$\gamma$-lactone | $2.71 \times 10^{-5}$ | 61 |

### 3.3. Side groups

The effect on the reaction rate of the substitution of various alkyl side chain constituents is presented in Fig. 4a whilst that for hydroxyl side groups is presented in Fig. 4b and Table IV. In both cases the base lactone is $\gamma$-butyrolactone, which is also shown for comparison. Similar data is shown in Fig. 4c and Table IV for hydroxyl groups on the 6-member ringed D-glucono-$\delta$-lactone. The effect of a carbonyl side group is shown in Fig. 4d using $\alpha$-acetyl-$\gamma$-butyrolactone.

### 3.4. Coagulant concentration

This was investigated using D-gulonic-$\gamma$-lactone. Whilst the effect was established at a range of temperatures, the direct influence of temperature is reported in the next subsection and hence the results in Fig. 5 are presented at the single value of 25°C. It can be seen that larger quantities of lactone favour a more rapid initial decrease in suspension pH, a lower pH minima and lower equilibrium values. In addition, longer processing intervals are required to reach these states.

### 3.5. Temperature

Fig. 6 presents the effect of temperature on the evolution of suspension pH at a constant concentration of D-gulonic-$\gamma$-lactone. As for concentration, it can be seen that a higher temperature favours a more rapid initial decrease in suspension pH, a lower pH minima and lower equilibrium values. However, unlike the results for concentration, shorter durations were required to reach these states.

## 4. Discussion

### 4.1. Effect of carboxylic acid derivative sub-classification

The reason behind the variations in the rate of pH decrease shown in Fig. 2 is clearly the rate at which the coagulant hydrolyses. Whilst it is known that low molecular weight

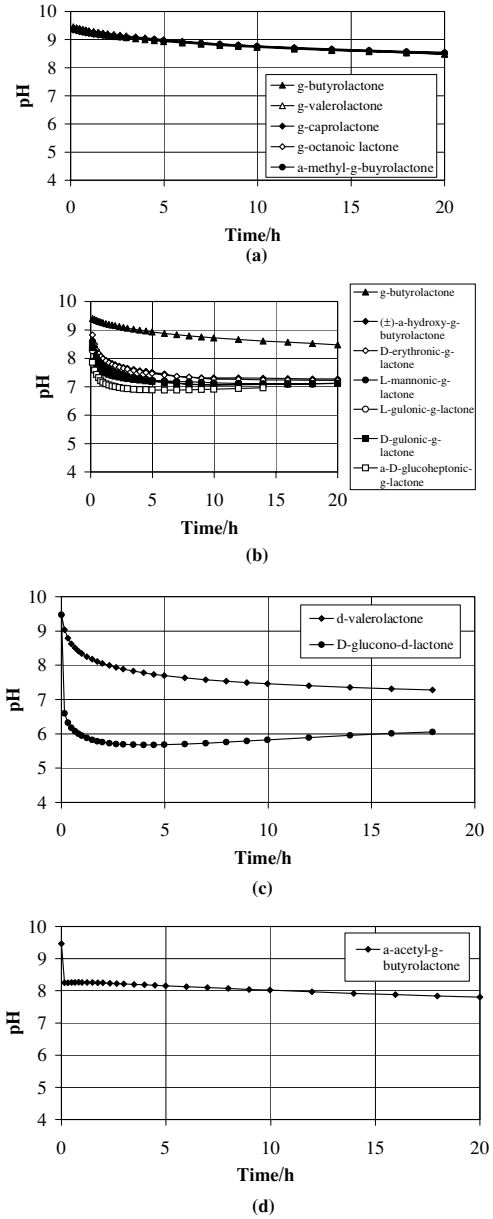


*Figure 4* (a) Effect of alkyl substituted side groups on suspension pH for a 5-membered ring lactone. (b) Effect of hydroxyl containing side groups on suspension pH for a 5-membered ring lactone. (c) Effect of hydroxyl containing side groups on suspension pH for a 6-membered ring lactone. (d) The effect of a carbonyl side group on suspension pH via the use of $\alpha$-acetyl-$\gamma$-butyrolactone.

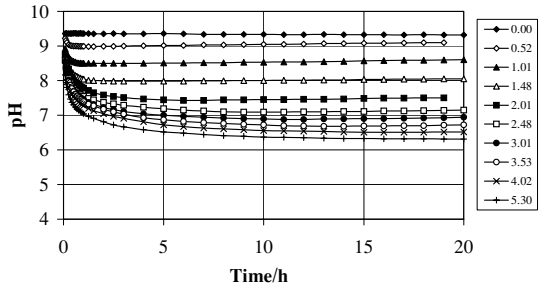


*Figure 5* The effect of concentration dependence on suspension pH via the use of D-gulonic-$\gamma$-lactone at 25°C.

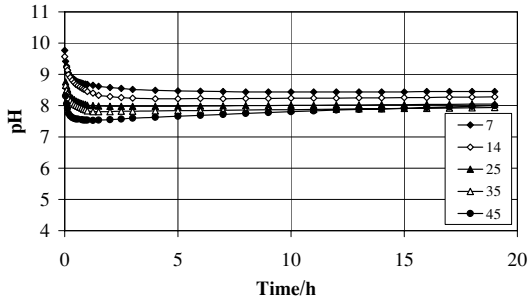


*Figure 6* The effect of temperature on suspension pH via the use of D-gulonic-$\gamma$-lactone at a concentration of $2.5 \times 10^{-5}$ mol $g^{-1}$.

anhydrides react violently with water, esters and amides react much more slowly.

The mechanism for the formation of the carboxylic acid product is nucleophilic substitution on the carbonyl carbon via an addition - elimination pathway, Fig. 7a. Whilst both steps can effect the rate of reaction, in general it is the first step that is rate determining [28]. Two factors that influence the rate of hydration are the free energy of reaction, $\Delta G$, and the magnitude of the activation free energy, $\Delta G^{\ddagger}$. The latter is affected by the phenomenon of resonance stabilisation; an electron pair contributes to the simultaneous bonding of more than two nuclei such that they become delocalised. This leads to the stabilisation of chemical structures and a modification of the atomic bond strength. As applied to the carboxylic acid derivatives, Fig. 7b, resonance interaction between the departing group and the carbonyl group results in a lowering of the energy associated with the ground state (reactants). Similarly, the nature of the departing group affects the free energy of reaction, $\Delta G$, though it does not influence $\Delta G^{\ddagger}$. The group departs with the electron pair by which it was originally bonded to the carbonyl carbon, the ease with which it can accommodate these electrons determines its stability. Weak bases, the conjugate bases of strong acids, are therefore good departing groups because they are able to accommodate the electron pair effectively. The stabilisation of the reactants and products brought about by

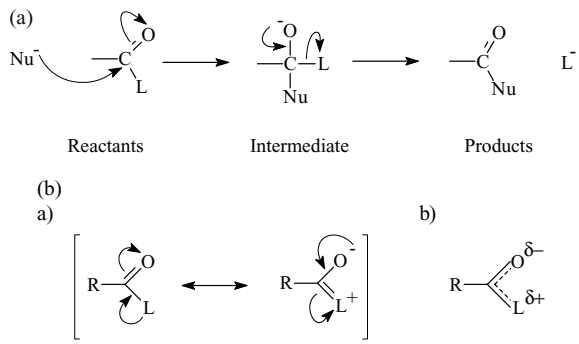


*Figure 7* (a) Generalised reaction mechanism for nucleophilic attack at a carbonyl carbon. (b) Resonant interactions occurring within carboxylic acid derivatives, a) extreme resonant forms indicating maximum charge separation and bond nature limits, b) true hybrid structure.

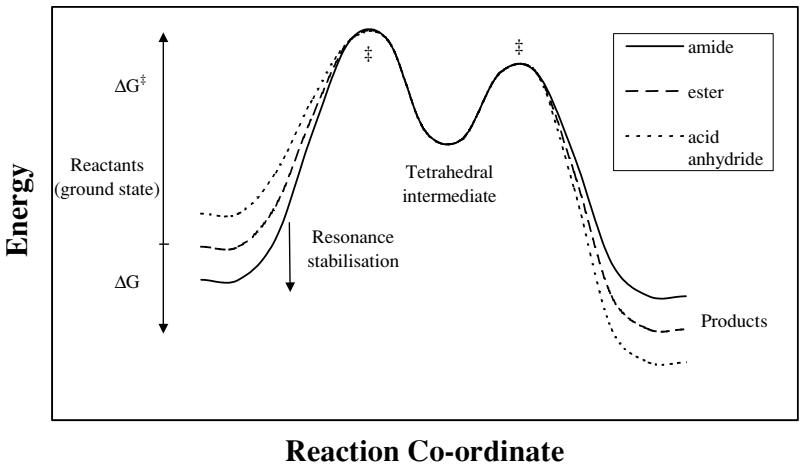


*Figure 8* Schematic energy profile diagram for nucleophilic substitution of linear amides, esters and acid anhydrides showing the relationship between ground, tetrahedral intermediate and transition states (‡), together with$\Delta G$ and $\Delta G^{\ddagger}$.

resonance stabilisation and the ability to accommodate electrons respectively are best illustrated graphically on an energy profile diagram, Fig. 8.

Amides are the least reactive derivatives because of the significant contribution of dipolar resonance stabilising the ground state. However at the transition stage, resonance stabilisation is lost [28]. This results in a high $\Delta G^{\ddagger}$ and a carbon - nitrogen bond that possesses significant double bond characteristics. Furthermore, the $^{-}NH_2$ departing group is strongly basic and so doesnot readily accept electrons. As a result the driving force for reaction is also low. The fundamentally slow coagulation rate associated with amide compounds rendered these additives ineffective for *in-situ* coagulation at acceptable rates. In contrast, resonance stabilisation at the carbonyl carbon within acid anhydrides is the lowest for the reagents investigated within this study. Although the oxygen can still 'push' electrons towards the carbon, the overall effect is diminished because of the presence of two carbonyl carbons. This results in a high ground state energy, low $\Delta G^{\ddagger}$ and a carbon - oxygen bond that possesses minimal double bond characteristics. In addition, the $RCO_2^{-}$ departing group is a weakly basic group that readily accepts electrons, consequently the driving force for reaction is high. The conclusion is that acid anhydrides would be ineffective for *in-situ* coagulation moulding because they are simply too reactive.

Esters are open chain molecules whilst lactones are closely related cyclic analogues, both are stabilised by resonance only to a modest extent. Accordingly, they possess an intermediate ground state energy, $\Delta G^{\ddagger}$ and double bond character relative to amides and acid anhydrides. The $^{-}OR$ functionality, which affects the driving force, also exhibits an intermediate stability. It is interesting to note, however, that the lactone yielded a faster rate of coagulation than the ester. A general comparison of the kinetic hydrolysis data available in the literature for these two types of compound showed that the presence of the ring structure resulted in kinetics that were always at least as fast, and could be faster by factors exceeding a million depending on the lactone structure. Thus these compounds were considered the best option for *in-situ* coagulation with the precise choice of lactone being decisive in establishing the optimal processing properties.

## 4.2. Effect of ring size

Figure 3 shows that the size of the ring has a marked effect on the rate of hydrolysis, and hence coagulation, exhibited by the lactone; a remarkably similar trend was obtained by Huisgen and Ott [26], Table V, who studied the addition of sodium hydroxide to unbranched lactones. The rates observed are attributable to several factors that influence the ground and intermediate states. Whilst each may play a role in the reactions of any given lactone, no single factor accounts for all the observations.

### *4.2.1. Factors effecting the ground state energy*

Lactones comprised of relatively small rings contain a large amount of strain energy that contributes to an

TABLE V Hydrolysis rate constants for lactones of different ring sizes relative to $\gamma$-butyrolactone, a) using sodium hydroxide nucleophile in 60:40 dioxane/water solvent at 0°C [26] and b) in the present work using ceramic suspensions at 25±1°C

| Lactone | Ring size | Relative hydrolysis rate constant[a] | Relative hydrolysis rate constant[b] |
|---|---|---|---|
| $\beta$-propyrolactone | 4 | 8.10 | 8.32 |
| $\gamma$-butyrolactone | 5 | 1 | 1 |
| $\delta$-valerolactone | 6 | 37.16 | 29.9 |
| $\varepsilon$-caprolactone | 7 | 1.689 | 0.98 |
| $\zeta$-heptanolactone | 8 | 2.36 | - |
| $\eta$-octanolactone | 9 | 0.07 | - |

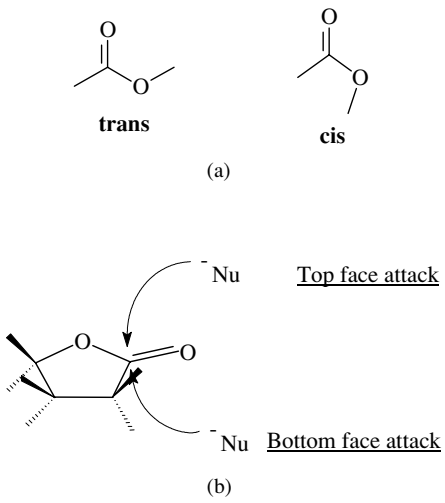


*Figure 9* (a) Cis and trans configurations of the ester function. (b) Definition of nucleophilic attack at the top and bottom faces of five membered lactone rings. The solid and dashed wedges symbolise the spatial positioning of bonds; solid wedges donate bonds that protrude out of the plane of the lactone ring, whereas dashed wedges represent bonds protruding into the plane.

increase in the ground state energy of the reactants. This ring strain may originate from several sources [25]:

- Lactone molecules with a ring size of less than 8 to 10 atoms are forced into a high energy cis configuration, whilst larger ring sizes (and open chain esters) adopt the lower energy trans configuration, Fig. 9a. The difference in energy arises from the nullifying effect of the dipole moment orientations present within the trans configuration, but absent in the cis.
- Due to the nature of the units comprising the rings, they are not geometrically planar but are best described as 'puckered'. Furthermore, in order to adopt a ring configuration the bond angles are slightly distorted from their idealised angles. These distortions are greatest in 4-and 6-membered rings, whilst it is considerably less in 5-membered rings [28].

#### *4.2.2. Factors effecting the transition and intermediate states*

In addition to increasing the ground state energy, ring strain factors may also influence the cyclic transition state. Direct comparison of hydrolysis rates is therefore complicated by the fact that energy changes between the transition states occur in addition to the ground states differences. However, the characteristics of the transition state play a much wider role in accounting for the hydrolysis rate accelerations observed. Intermediate formation results in a marked configurational change as a tetrahedral intermediate is formed from an initially planar carbonyl group, a modification that is accompanied by steric strains.

In the case of the 6-membered ring, formation of the tetrahedral intermediate produces a strain-free configuration. This combination of a stable intermediate with an unstable ground state, see above, results in the lowest $\Delta G$ and hence rapid reaction rates, a fact confirmed by the experimentally determined activation energy, Table III. The relatively fast hydrolysis of such $\delta$-lactones, under physiologically moderate conditions, is often exploited [31]. In contrast, in 5-membered butyrolactone the formation of the tetrahedral intermediate introduces strain into the structure. The combination of a stable ground state with destabilised intermediate results in the largest energy difference and hence the slowest rate, and the activation energy is high. Whilst the absolute energy values associated with both ground and intermediate states for the 7-membered ring are slightly higher than for the 5-membered ring, these differences are so similar in size that the overall outcome for $\Delta G^{\ddagger}$ is similar in the two cases and the activation energies are effectively the same, Table III. The situation for the 4-membered ring is such that the destabilising contributions for both reactant and intermediate are considerable, however they combine to generate a rate between the extremes of 5- and 6-membered ring behaviour.

An alternative factor that can reduce the intermediate energy is if the lactone undergoes hydrolysis via a different route, for example the elimination - addition pathway. Although not of significance to the current discussion of unbranched lactones, it will be relevant in a later section when the effect of carbonyl substituent side groups are discussed.

### 4.3. Alkyl side groups

Although the substitution of a methyl side chain was examined at two different sites and the effect of methyl through to propyl side chains at one site, Fig. 4a clearly shows that for a 5-membered ring the substitutions did not significantly affect the reaction rate. This may be explained by the fact that the presence of the alkyl group does not significantly affect the structure of the reactants or reaction intermediates. The non polar, saturated nature of the group excludes any electrostatic or resonance effects. Furthermore, the groups investigated were not sufficiently bulky in size to facilitate steric hindrance, such that no new rate influencing factors were introduced by the presence of the side groups.

### 4.4. Hydroxyl side groups

Fig. 4b and Table IV showed that the number of OH groups on side chains influenced the coagulation rate. Whilst it is known that hydroxyl groups themselves are acidic and capable of undergoing dissociation it is unlikely that this mechanism in isolation accounts for the increased hydrolysis rates because the pKa values associated with the ionisation of alcohols is high ($\sim$15), so that the reaction is somewhat unfavourable. Rather, it is proposed that the shape of the molecule is critical. Although the lactone ring as a whole is puckered, the carbonyl group within the ring is planar. In the discussions up to this point preferential nucleophilic attack on one side of the plane has been insignificant because of the non-enantiomeric nature of

*Figure 10* A molecular model depicting the bottom face approach of nucleophilic water to (R)-$\alpha$-hydroxyl-$\gamma$-lactone. The light green sticks indicate bonds and the coloured spheres represent carbon (black), oxygen (red) and hydrogen (white) atoms respectively.

compounds. However, as shown in Fig. 9b, for the planar five-membered lactones examined in this part of the work it is possible to arbitrarily define attack as being at the top or bottom faces of the structure. Based on this concept, it is now possible to explain the order for the rate of coagulation shown in Table IV.

Whilst ($\pm$)-$\alpha$-hydroxy-$\gamma$-butyrolactone is the slowest of the hydroxyl-bearing compounds, it can be seen that the presence of the single hydroxyl group adjacent to the carbonyl carbon undergoing attack has a profound accelerating influence on the rate of coagulation compared to the base lactone, $\gamma$-butyrolactone. To explain this, it is necessary to visualise the range of spatial orientations that the molecule can adopt by bond rotation. Fig. 10 illustrates the approach of water to an (R) form configuration.[7] It can be seen that rotation around the bond, as indicated by the curved arrow, results in a series of molecular conformations. It is suggested that the presence of hydrogen bonding interactions between the O and H atoms in the lactone with the H and O atoms in the water not only accounts for the preferred conformations, but also stabilises the transition state. As stated earlier, the latter represents a local point of highest energy, the magnitude of which, $\Delta G^{\ddagger}$, governs the rate of reaction. Hydrogen bonding stabilises the transition state by reducing the interaction energy associated with it and, as a result of the lower energy barrier, a faster reaction rate transpires. The experimentally determined activation energies in Table IVb appear to substantiate this theory. Although this discussion focused on nucleophilic attack on the bottom face of the (R) configuration, a similar situation would arise for the

[7]Note: the ($\pm$) designation in the name of the lactone indicates that the compound is comprised of 50% (R), where the bond protrudes towards the ring, and 50% (S), where the bond points away from the ring.

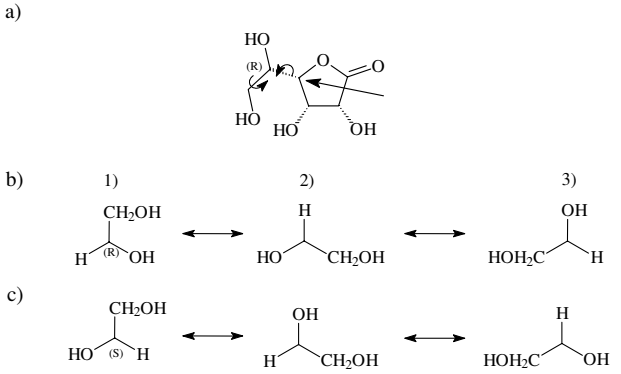


*Figure 11* (a) Bond rotation in L-mannonic-$\gamma$-lactone, (b) Representation of the conformations that may be produced by viewing along the bond indicated by the solid arrow in (a) for L-mannonic-$\gamma$-lactone and (c) D-gulonic-$\gamma$-lactone.

(S) case with top attack. Since the two forms are present in equal ratio, there is no advantage to an attack at either face.

It can be seen that the addition of a second hydroxyl group in D-erythronic-$\gamma$-lactone results in minimal further increase in coagulation rate. The most likely explanation is that the additional distance from the carbonyl carbon hinders supplementary hydrogen bonding interaction. It is interesting to note that the stereochemistry of this lactone is markedly different from the previous one, in that the position of both hydroxyl groups is fixed and point towards the lactone ring. In this case attack at the bottom face would lead to favourable interactions between the nucleophile and the OH side groups.

The next three lactones, L-mannonic-$\gamma$-lactone, D-gulonic-$\gamma$-lactone and L-gulonic-$\gamma$-lactone, all possess 4 OH groups. For L-mannonic-$\gamma$-lactone, two of them are identical to those in D-erythronic-$\gamma$-lactone, with the remaining two on a constituent group branched onto the adjoining carbon. The result is a further increase in coagulation rate. At a first glance the acceleration would appear to be somewhat larger than expected, however a variety of conformations resulting from bond rotation can be adopted by the supplementary OH groups to enhance hydrogen bonding with incoming water. Viewing and rotating along the bond indicated by the solid arrow in Fig. 11a allows visualisation of the conformations that may be adopted, Fig. 11b. The effect of the (arbitrarily designated) conformer positions, 1, 2, 3, on the interaction between the OH entity on the constituent group and nucleophilic water is highlighted in Table VI. It can be seen that conformer positions 1 and 3 promote favourable, transition state stabilising, lactone - water interactions.

D-gulonic-$\gamma$-lactone is a diastereoisomer of L-mannonic-$\gamma$-lactone with a configurational difference on the hydroxyl-rich side group, which in the case of D-gulonic-$\gamma$-lactone is (S), whereas it is (R) for L-mannonic-$\gamma$-lactone. A small increase in coagulation rate arises as a result of this subtle difference. This can be

TABLE VI Hydrogen bond interactions between OH side group constituents and water as a function of conformer position for L-mannonic-$\gamma$-lactone and D-gulonic-$\gamma$-lactone. A significant interaction is represented by √.

| Side group | L-mannonic-$\gamma$-lactone | | | D-gulonic-$\gamma$-lactone | | |
|---|---|---|---|---|---|---|
| | 1 | 2 | 3 | 1 | 2 | 3 |
| $CH_2OH$ | | | √ | | | √ |
| OH | √ | | | | | √ |

explained by noting the conformers adopted, Fig. 11c; Table VI shows that the interaction produced by conformation 3 is particularly strong since it is only in this conformation that both hydroxyl groups simultaneously occupy a spatial arrangement that maximises interaction with nucleophilic water. L-gulonic-$\gamma$-lactone is the mirror image of D-gulonic-$\gamma$-lactone and as a result of the enantiomeric match, and since water is achiral, identical hydrolysis rates are expected and observed.

Based on these conformational studies, it was predicted that $\alpha$-D-glucoheptonic-$\gamma$-lactone should result in a further, substantial increase in reaction rate. The structure of this molecule is similar to D-gulonic-$\gamma$-lactone except it possesses an additional $CH_2OH$ unit bonded onto the end of the hydroxyl-rich side chain. It was suspected that the latter would further encroach upon the attacking water, bolstering the reaction rate, and in addition molecular models indicated that the supplementary unit could adopt spatial orientations to place it in close proximity to the water. The results in Fig. 4b and Table IV substantiate this theory. This example clearly indicates that placing an extra hydroxyl unit at a location that may initially seem remote can have a profound influence on the hydrolysis rate of the reaction occurring on the other side of the molecule due to the favourable conformations that may be adopted.

The data in Fig. 4c and Table IV for the six-membered D-glucono-$\delta$-lactone allows a direct comparison between the hydrolysis results obtained in the current work and the literature. Skou et al. [32] obtained a rate constant of $4.59 \times 10^{-5}$ $s^{-1}$ by employing a pH static method at 25°C, which compares favourably with the value of $2.71 \times 10^{-5}$ $s^{-1}$ at the same temperature in the present work. Similar agreement also exists for the activation energy; Skou et al and Sawyer et al [33] obtaining values of 61 and 63 kJ $mol^{-1}$ respectively, which compare very favourably with the 61 kJ $mol^{-1}$ obtained in the current work. These results give confidence in the other values presented in this publication.

## 4.5. Carbonyl side group

It can be seen from Fig. 4d that the time dependent pH profile produced by $\alpha$-acetyl-$\gamma$-butyrolactone relative to all the previous lactones is entirely different; in this case the structure of the lactone promotes coagulation via the elimination - addition mechanism. The proton adjacent to the carbonyl group is readily lost and this accounts for the rapid initial pH decrease. Proton elimination is facilitated by the formation of an intermediate that is highly stabilised by resonance. For all the other lactone compounds investigated in this study, the side groups do not promote resonance stabilisation so that proton generation is not facilitated. Rearrangement of the intermediate promotes the formation of a ketene intermediate (=C=O) that is subsequently attacked by the nucleophile in the addition step.

## 4.6. Coagulant concentration and process temperature

The ideal coagulation rate for the formation of ceramic components is a compromise between two competing factors. If the additives hydrolyse too quickly then the homogeneity of the rapidly coagulating suspensions will be lost whilst if the additives coagulate too slowly then the processing times become uneconomically long. Based on this situation, D-gulonic-$\gamma$-lactone was identified as an effective additive because it demonstrated a natural balance between reactivity and stability and hence it formed the basis of a more detailed, systematic evaluation of the effect of coagulant concentration and process temperature. This lactone was selected over its mirror image enantiomer, L-gulonic-$\gamma$-lactone, on the basis of the large cost differential between the two compounds.

### *4.6.1. Effect of concentration*

The results shown in Fig. 5 indicate that a time dependent pH decrease is initially apparent, after which a marginal pH increase is noted prior to the establishment of equilibrium conditions. The hydrolysis of the D-gulonic-$\gamma$-lactone results in the production of D-gluconic acid, which subsequently ionises to form $H^+$. Since the latter is time dependent, the evolution of the suspension pH exhibits the same dependency. The presence of the $H^+$ then coagulates the suspension as a result of the neutralisation of the negative charges associated with the NHPA dispersant. The advantage of this *in-situ* formation of acid is that the lactone reagent can be thoroughly mixed into the suspension without a significant change in suspension properties. Consequently, as the internal reaction proceeds the suspension is homogeneously coagulated. The subsequent slow pH increase is believed to be due to the time dependent neutralisation of the negative charges on the polyelectrolyte by the residual $H^+$ ions. Fig. 5 also shows that, as intuitively expected, both the extent and rate of coagulation are affected by the coagulant concentration. Larger additions favour a more rapid initial decrease and a lower equilibrium suspension pH since a larger concentration of acid is produced.

An attempt was made to obtain quantitatively the equilibrium constant for the overall reaction using the equilibrium pH values. Such information would have been valuable in establishing the extent to which the reactants were converted into products. However, the value, which

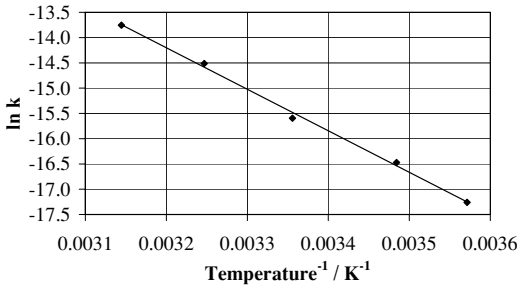


*Figure 12* Arrhenius plot for the coagulation of an 81 wt%, 1.4 mg $g^{-1}$ NHPA containing suspension using D-gulonic-$\gamma$-lactone.

should have been constant, varied depending upon the amount of lactone present. The reason for this was the number of side reactions occurring. Most notably, acidic protons will have been consumed by combination with the negatively charged polyacrylate and surface hydroxyl groups on the alumina during the coagulation process. Other side reactions will have included the presence of sodium impurities on the alumina particles, dissociation of hydroxyl constituents in the lactone, decomposition of ammonium ions and the direct addition of water to the polyelectrolyte. These simply introduced too many unknown variables to allow accurate values for the equilibrium constant to be obtained.

### *4.6.2. Effect of temperature*

Fig. 6 shows that marked differences in the rate and extent of coagulation can be achieved by changing the suspension temperature. For example, even before the lactone is added the initial suspension pH is lower at higher temperatures; this is mostly likely attributable to the temperature enhancement of the reaction $NH_4^+ \rightarrow NH_3 + H^+$. It can be seen in Fig. 6 that higher temperatures favour a more rapid initial decrease in suspension pH, a reduced pH minima and lower equilibrium values. Once again, these results may be explained by the speed and amount of acid produced by the hydrolysis reaction. Calculation of the Arrhenius temperature dependency, Fig. 12, shows a good fit to a linear trendline and reveals an experimental activation energy of 68 kJ $mol^{-1}$, a value that shows a reasonable match with the literature [23].

The effect of both concentration and temperature on the rheology of the coagulating suspension will be discussed elsewhere [34]. However, an additional observation pertinent to the pH minima and equilibria values, is that the pH of the suspension is always greater than 6. The significance of this is that it corresponds to the IEP of alumina particles coated with 1.4 mg/g NHPA [30]. Consequently, re-stabilisation of the alumina particles resulting from the generation of a positive surface charge at pH levels below the IEP is avoided. If this were to occur, it would be deleterious to the coagulation process because of the erosion of the formed structure.

## 5. Conclusions

It has been demonstrated that dispersed suspensions can be successfully coagulated in a time-dependent manner using the carboxylic acid derivative group of chemicals. These chemicals, amides, esters, lactones and acid anhydrides, which are initially inactive, hydrolyse over a period of time to produce carboxylic acids, which in turn cause the suspension to coagulate. As a result of the initially passive nature of these additives, they can be thoroughly mixed into the dispersion such that coagulation is homogeneously achieved internally.

These additives demonstrate a diverse range of coagulation rates, ranging from virtually ineffective to highly reactive. The inherent coagulation rate, which is determined by the nature of the atom bonded to the carbonyl carbon, can be accelerated by adding substituent hydroxyl groups. These side group entities can adopt a range of spatial arrangements, however certain conformations result in the formation of hydrogen bonds with the attacking water nucleophile. These favourable interactions stabilise the transition state and hence reduce the activation energy. Furthermore, for cyclic compounds the size of the ring also exhibits a profound influence on the coagulation rate, with several contributory factors that affect the ground and transition state energies responsible for the observed trends.

In addition to the chemical nature of the additive, the progression of coagulation is also critically dependent on the concentration of coagulant and temperature. Increasing either greatly accelerates the extent and rate of coagulation.

## Acknowledegments

The authors would like to acknowledge gratefully the support of the Engineering and Physical Science Research Council (EPSRC) and Dytech Corporation Ltd, both in theUK.

## References

1. D. J. SHAW, Introduction to Colloid and Surface Chemistry, Chapters 7 & 8, Butterworths, 1992.
2. R. G. HORN, *J. Am. Ceram. Soc.* **73**(5) (1990) 1117.
3. F. F. LANGE, *J. Am. Ceram. Soc.* **72**(1) (1989) 3.
4. F. F. LANGE, B. V. VELAMAKANNI, J. C. CHANG and D. S. PEARSON, Proc of the 11th Ris$\phi$ Int. Symp. on Metall. & Mat. Sci. (1990) 57.
5. R. E. COWAN, Treatise on Materials Science and Technology, Vol. 9, Ceramic Fabrication Processes, F.F.Y. Wang (Ed.), Academic Press (1976) 153.
6. S. W. SOFIE and F. DOGAN, *J. Am. Ceram. Soc.* **84**(7) (2001) 459.
7. O. O. OMATATE, *Am. Ceram. Soc. Bull.* **70**(10) (1991) 1641.
8. T. J. GRAULE and L. J. GAUCKLER, *Industrial Ceramics* **16**(1) (1996) 31.
9. B. V. VELAMAKANNI, *Langmuir* **6**(7) (1990) 1323.
10. J. C. CHANG and F. F. LANGE, *J. Am. Ceram. Soc.* **77**(1) (1994) 19.
11. B. V. VELAMAKANNI, Ceramic Transactions 26, M.J. Cima (Ed.), *Am. Ceram. Soc.* (1992) 187.
12. H. GOEL, Ceramic Transactions 62, J. J. Kingsley (Ed.), *Am. Ceram. Soc.* (1996) 241.

13. C. H. SCHILING and H. GOEL, *J. Environmental Polymer Degradation* **3**(3) (1995) 153.
14. T. K. YIN and I. A. AKSAY, Ceramic Transactions 1, G.L. Messing (Ed.), *Am. Ceram. Soc.* (1988) 654.
15. L. BERGSTRÖM, *J. Am. Ceram. Soc.* **75**(12) (1992) 3305.
16. J. DAVIES and J. G. P. BINNER, *J. Eur. Ceram. Soc.* **20** (2000) 1555.
17. J. CESARANO, I. A. AKSAY and A. BLEIER, *J. Am. Ceram. Soc.* **71**(4) (1988) 250.
18. J. LYKLEMA and G. J. FLEER, *Colloids and Surfaces* **25** (1987) 357.
19. P. A. WILLIAMS, P. HARROP and G. O. PHILLIPS, The Effect Of Polymers On Dispersion Properties, Th. Tadros (Ed.), Academic Press, (1982) 361.
20. T. J. GRAULE and L. J. GAUCKLER, *Deutsche Keramische Gesellschaft*, **71** (1994) 317.
21. F. H. BAADER, *Industrial Ceramics* **16**(1) (1996) 36.
22. G. V. FRANKS and F. F. LANGE, *J. Am. Ceram. Soc.* **78**(5) (1995) 1324.
23. S. J. BENKOVIC, A. J. KIRBY and R. J. E. TALBOT, Comprehensive Chemical Kinetics, 10, C. H. Bamford, and C. F. H. Tipper (Eds.), Elsevier Publishing Company, 1972.
24. K. B. WIBERG, R. F. WALDRON, G. SCHULTE and M. SAUNDERS, *J. Am. Chem. Soc.* **113** (1991) 971.
25. K. B. WIBERG and R. F. WALDRON, *J. Am. Chem. Soc.* **113** (1991) 7697.
26. R. HUISGEN and H. OTT, *Tetrahedron* **6** (1959) 253.
27. W. P. JENCKS and J. CARRIUOLO, *J. Am. Chem. Soc.* **82** (1960) 1778.
28. E. T. KAISER and F. J. KEZDY, Progress in Bioorganic Chemistry, 4, E. T. Kaiser and F. J. Kezdy (Eds.), Wiley Interscience, (1976) 239.
29. G. V. BOYD, The Chemistry of Acid Derivatives, Supplement B, Part 1, Chapter 10, S. Patai (Ed.), John Willey and Sons (1979) 491.
30. J. DAVIES and J. G. P. BINNER, *J. Eur. Ceram. Soc.* 20 (2000) 1539.
31. S. BANON and J. HARDY, *J. Dairy Research* **58** (1991) 75.
32. E. M. SKOU and T. JACOBSEN, *Acta Chemica Scandinavica* **36** (5) (1982) 417.
33. D. T. SAWYER and J. B. BAGGER, *Am. Chem. Soc.* **81** (1959) 5302.
34. J. G. P. BINNER, I. SANTACRUZ and A. M. MCDERMOTT, accepted for publication in *J. Am. Ceram. Soc.*, in press.

*Received 29 April*
*and accepted 13 June 2005*